Kathmandu University Journal of Science, Engineering and Technology, Vol. X, No. X, Month Year

Kathmandu University
Journal of Science, Engineering and Technology

Development of a high and low temperature Agro-dryer using biomass and an integrated moisture laden extractor fans

Francis Onoroh*[a], Nehemiah Sabinus Alozie[a], Uche Paul Onochie[b], and Efetobore Justice Esiri[a]

[a]Department of Mechanical Engineering, University of Lagos, Akoka, Lagos, Nigeria.
[b]Department of Mechanical Engineering, Southern Delta University Ozoro, Nigeria.

Abstract

Agricultural produce spoilage from microbial activity is a major course of concern. One of the means to reduce microbial activity is to reduce the amount of moisture content in crops. This is most often achieve by sun drying or using cabinet dryer. However due to varied drying temperature and moisture contents of crop this research have developed and tested a high and low temperature cabinet suitable for drying crops with high and low moisture contents requiring different air temperature in order to retain the nutritional value of agricultural produce. The drying rate for the respective produce are 0.08875, 0.02, 0.1275, 0.025, 0.07 and 0.07 kg/h for tomatoes, pepper, onions, bitter-leaf, fish and plantain respectively, with the high temperature chamber experiencing higher drying rates than the low temperature chamber due its higher temperature. The maximum recorded temperature in the high and low chamber are 69 °C and 52 °C, 60 °C and 45 °C, 75 °C and 55 °C respectively for day 1, day 2 and day 3 of testing. Peak high-chamber efficiency was 49% and consistently exceeded the low-chamber peak of 35%. This demonstrates that the developed high and low temperature cabinet dryer is both functional and efficient for multi-crop drying application.

Keywords: Temperature; Moisture content; Drying rate; Efficiency; Chamber.

1. Introduction

Over the years, post-harvest agricultural produce losses has been a consistent challenge to farmers who toil day and night to feed the astronomical increase in world population [1]. As a way out, farmers resort to drying to increase the shelf life of their produce while also retaining their nutritional value [2]. However, open sun drying remains the norm, despite its inefficiency and associated contamination due to rodent attack and other contaminants inherent in atmospheric air and variability of atmospheric weather conditions [3, 4, 5]. Cabinet dryers leverage on these demerits of open sun drying by providing an enclosed structure to shield the produce from rodents, insects and other contaminants present in the air. The cabinet dryers draw their energy either from combustion of biomass or natural gas, solar energy and via electrical heating elements, or a combination of both, usually termed hybrid, with varying degrees of effectiveness and relative cost of operation [6]. Biomass energy, derived from agricultural residues such as rice husks and wood, provides a sustainable and cost-effective fuel source [7]. The current developed cabinet dryer has a high and low temperature chamber particularly suited for drying agricultural produce with high and low moisture content that are particularly susceptible to drying temperatures, with air circulation enhancement via a forced through blower and an extractor fan.

Onoroh et al. [3] developed a single cabinet dryer for drying of multiple agricultural produce using biomass as energy source. The drying air is indirectly heated in a heat exchanger and efficiency of 45% was achieved while drying tomatoes, okra, and bitter leaves. Murugan et al. [4] carried out an overview of industrial and small-scale dryers using biomass with emphasis on economic and sustainability aspects. They identified poor air circulation as a major cause of uneven drying and recommended structural improvements and better airflow with a view to improving performance of cabinet dryers. Mahajan et al. [8] designed and analysed a turmeric solar-biomass dryer incorporating solar absorber, biomass burner, blower, drying cabinet, and exhaust heat exchanger. The performance of the dryer was simulated using ANSYS Fluent yielding temperature distribution range of 60–65 °C at an airflow velocity of 2 m/s. Kumara et al. [5] developed a dual-heat dryer combining biomass and solar energy. Their dryer achieved a drying air temperature in the range of 40 °C and 110 °C while drying drumsticks, bitter gourd, papaya, mango, lemon grass, and mushroom with natural convective airflow.

Sinon et al. [9] conducted an experimental study of a dryer suitable for drying fruits and vegetables. Test results showed that the dryer has an efficiency of 10.76%, while combusting biomass connected to a water-air heat exchanger reducing the moisture content from 93.8% to 12% in sixteen hours of operation. Akowuah et al. [10] investigated the effect of drying temperature on kernel damage and viability of maize, and evaluated the impact of drying temperatures on a solar-biomass dryer. The moisture content of maize was reduced from 22.8% to a desirable value of 12.8% with drying air temperatures ranging from 44.4 °C to 52.8 °C, with the goal of reducing stress cracking. Ezurike et al. [11] designed and performed a numerical analysis on a semi-automated biomass-powered multipurpose dryer with temperature control sensor predetermined at 67 °C. The peak moisture removal rate of the sample was 0.0066 kg/h, while the sample attained 40% moisture concentration of its initial value; 90% mass content removal of the initial mass of the sample was achieved at the end, with a simulation time of 240 s during testing.

From the review, several works have investigated biomass cabinet dryers; however, little emphasis has been placed on efficient air circulation that guarantees effective moisture removal and even

*Corresponding author. Email: fonoroh@unilag.edu.ng

drying, and on the different temperature requirements of specific crops. Thus, this research has effectively developed and tested a high and low temperature cabinet dryer suitable for drying a wide variety of crops of varying degrees of moisture content, with a combination of forced-through and drawn-out air, with biomass as thermal energy source and solar energy as electrical energy source, with an integrated indirect heat exchanger.

2. Materials and methods

The agro-dryer is constructed as a two-chamber drying system, comprising a high-temperature and low-temperature zone, fabricated using angle bar for structural integrity lined with mild steel sheet. It includes a detachable charcoal-fuelled combustion chamber integral with a heat exchanger. To facilitate forced convection, a 24 V DC-powered blower circulates ambient air through the heat exchanger and into the dryer after indirect heating by the combustion of biomass. A 24 V extractor fan on top of the low temperature chamber facilitates evacuation of moisture-laden air from the dryer; both the fan and blower are powered using solar energy via photovoltaic panels and storage batteries. The drying chambers house perforated mesh trays arranged in tiers (Tray 1, Tray 2, and Tray 3), enabling uniform distribution of heated air and efficient contact with the crop surfaces. Figure 1 shows the schematic of the dryer. The high temperature chamber ensures quick removal of moisture from high moisture content products while the low temperature chamber is used for heat-sensitive products and ensures slow evaporation of moisture without degrading their nutrients. The design has been made in this way so that the dryer can be used to dry both high and low moisture content products without nutrient degradation while using the same source of energy, thereby increasing the efficiency of the dryer and reducing energy consumption.

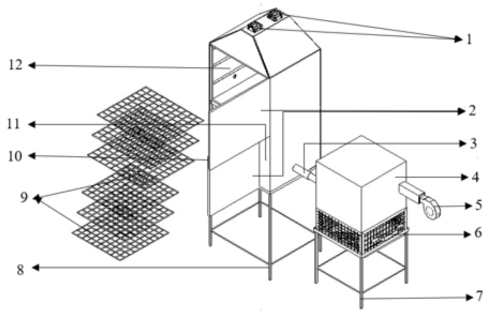

Figure 1: Dryer components and assembly

Dryer Components and Assembly. Part list: 1. Extractor fans, 2. Dryer doors, 3. Detachable connecting pipe, 4. Heat exchanger, 5. Blower, 6. Combustion chamber, 7. Combustion chamber stand, 8. Dryer stand, 9. Drying trays, 10. High chamber, 11. Air plenum, 12. Low chamber.

2.1. Blower and extractor selection

The heat energy required to dry agricultural products is directly linked to the thermal capacity of the air stream used in the drying chambers. This energy is supplied by the combustion of biomass in a high-efficiency combustion chamber. The drying air supplied by the blower absorbs thermal energy as it passes through the heat exchanger, resulting in a temperature increase. The energy balance governing this heat transfer is expressed as Equation (1) [12, 13]:

$$m_b \, \mathrm{LHV} = m_a c_a (T_1 - T_2) \times \eta_c \tag{1}$$

where m_b is the mass of biomass (kg); LHV is the lower heating value of biomass (kJ/kg); m_a is the mass flow rate of drying air (kg/s); c_a is the specific heat capacity of air (kJ/kgK); T_1 is the heat exchanger inlet temperature (K); T_2 is the heat exchanger exit temperature (K); η_c is the thermal efficiency of the combustion. The mass flow rate of drying air is determined using Equation (2) [14]:

$$m_a = Q \times \rho_a \tag{2}$$

where Q is the blower flow rate (m^3/s) and ρ_a is the air density at drying conditions (kg/m^3). Table 1 gives the specification of the selected blower based on its static pressure and flow rate.

Table 1: Blower specification.

Parameter	Value
Maker	Lawrence Brown
Model	RG133-46/24-200
Voltage	24 V DC
Power	40 W
Flow rate	0.05286 m^3/s
Static pressure	154.4 Pa

For ease of drying air circulation and to overcome pressure loss in the dryer, two extractor fans are installed on top of the low temperature chamber, ensuring facilitation of the removal of moisture-laden air from the chamber. The specification of the deployed extractor fans is given in Table 2. These fans were chosen for their low power consumption and matching flow rate to the blower.

Table 2: Specification of extractor fan.

Parameter	Value
Maker	Delta Electronics, INC
Model	FFB0924EHE
Voltage	24 V DC
Power	12 W
Flow rate	0.052 m^3/s
Static pressure	166 Pa

2.2. Heat exchanger design

The heat exchanger serves as the critical interface for indirect thermal energy transfer from the combustion chamber to the drying chamber, enabling clean, food-safe heating without introducing combustion gases. Its role is to capture and transmit heat from hot flue gases to the airflow that circulates through the drying system, ensuring consistent and efficient moisture removal. Figure 2 shows the internal geometry of the heat exchanger.

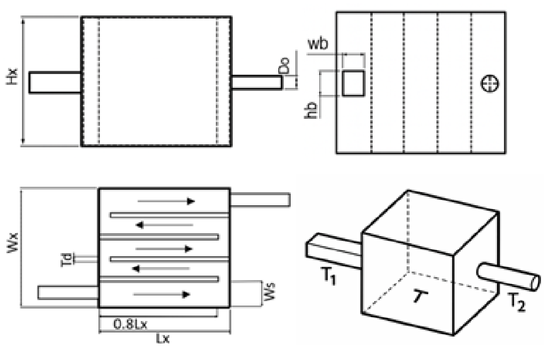

Figure 2: Drawing of the heat exchanger.

Table 3: Agricultural products drying parameters [15, 16, 17, 18, 19, 20, 21].

Dryer Chamber	Crop	MC_i (%)	MC_f (%)	T (°C)	t (hr)	m_w (kg/kg)	Q (kJ)
High-Temperature	Tomatoes	85–95	6–10	45–65	15–20	0.84	1898
	Onions	80–86	7–14	35–45	6–8	0.79	1785
	Fish	65–75	10–15	45–60	6–10	0.68	1602
Low-Temperature	Pepper	65–75	8–12	35–50	5–7	0.65	1469
	Bitter-leaf	80–90	5–12	35–50	4–6	0.80	1808
	Plantain	55–70	10–15	55–70	6–10	0.54	1220

MC_i and MC_f stand for initial and final moisture content (%).

The exchanger was fabricated using mild steel plate, chosen for its high thermal conductivity and structural stability. It features four vertical plates, each acting as a single pass, resulting in 5 parallel air passes within the heat exchanger, making the design more compact, resulting in increased contact surface area and improved heat transfer. An outer shell encloses the drying air, which is heated via conduction and convection. The basis of the design is the need to reduce the surface area of flow, thereby increasing the air velocity and turbulence, ensuring improvement in the overall heat transfer coefficient leading to enhanced thermal efficiency. During steady operation, the bottom plate of the heat exchanger remains at a quasi-fixed temperature due to continuous combustion of biomass beneath it. This constant high-temperature interface drives heat into the internal air volume through the exchanger walls. Each hot surface facing the airflow provides a path for heat transfer to the air. The rate of heat absorbed by the air can be determined from Equation (3) [12]:

$$Q = UA_o\Delta T_{lm} \tag{3}$$

where U is the overall heat transfer coefficient (W/m^{2}K); A_o is the surface area of flow (m^2); ΔT_{lm} is the log-mean temperature difference (K). The log-mean temperature difference is obtained using Equation (4):

$$\Delta T_{lm} = \frac{(T - T_1) - (T - T_2)}{\ln\left(\dfrac{T - T_1}{T - T_2}\right)} \tag{4}$$

where T is the heat exchanger bottom plate temperature (K).

2.3. High and low moisture content agricultural products

The efficiency and design parameters of the high and low agro-dryer are determined based on the moisture content, drying temperature, and required airflow rates of selected agricultural products. High-moisture crops, such as tomatoes (*Lycopersicon esculentum*), onions (*Allium cepa*) and herring fish (*Clupea harengus*), require higher drying temperatures to facilitate moisture removal [11]. In contrast, low-moisture crops, including bitter-leaf (*Vernonia amygdalina*), plantain (*Musa paradisiaca*), and pepper (*Capsicum* spp.), require gentler drying conditions to preserve quality and prevent excessive dehydration [3]. The high and low moisture content crops used for testing are depicted in Figure 3.

Table 3 details their initial and final moisture contents, drying temperature, drying time, dehydration per kg, and the quantity of heat energy required per fresh product.

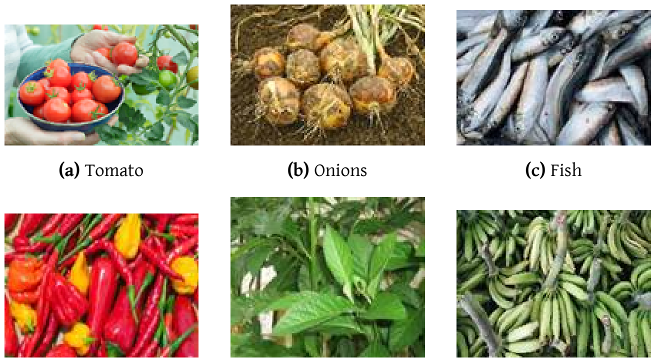

(a) Tomato **(b)** Onions **(c)** Fish

(d) Pepper **(e)** Bitter-leaf **(f)** Plantain

Figure 3: Experimental agricultural crops. Top row: high moisture crops . Bottom row: low moisture crops.

The products are grouped into chamber-specific drying pairs. High moisture content crops are placed in the high-temperature chamber while low moisture content crops are placed in the low-temperature chamber. The combined heat requirement represents the total energy needed per drying cycle for both chambers operating simultaneously. The pairing of these agricultural products is as shown in Table 4.

Table 4: Pair of crops in the chamber during drying.

Pair	High Chamber	Low Chamber	Q (kJ)
Pair 1:			
Tomato + Pepper	Tomato	Pepper	3367
Pair 2:			
Onion + Bitter-leaf	Onion	Bitter-leaf	3593
Pair 3:			
Fish + Plantain	Fish	Plantain	2822

The final moisture content of each crop is determined using the wet basis as expressed in Equation (5) [18, 22]:

$$\mathrm{MC} = \frac{w_w}{w_w + w_d} \times 100 \tag{5}$$

where w_w is the mass of water removed during drying (kg) and w_d is the final mass of the dried crop after drying (kg). The mass of water to be evaporated from any agricultural product is determined using Equation (6) [23, 24, 25]:

$$m_w = m_i \frac{\mathrm{MC}_i - \mathrm{MC}_f}{100 - \mathrm{MC}_f} \tag{6}$$

where m_i is the initial mass of the crop before drying (kg); MC_i is the initial moisture content (%); MC_f is the final moisture content (%).

Drying is a coupled heat and mass transfer process, where moisture migrates from the interior of a solid to its surface and is then removed by an air stream. In this system, the transfer of internal moisture is governed by Fick's Second Law of Diffusion, while external moisture removal is driven by thermal convection and airflow.

The rate at which moisture diffuses through the crop matrix is quantified by the effective moisture diffusivity, which captures the collective effect of molecular diffusion, capillary flow, and vapour diffusion. This parameter is highly temperature-dependent and varies with the physical structure, moisture content, and composition of the material being dried.

The diffusivity is governed by Equation (7) [20, 26, 27]:

$$D_{\text{eff}} = \frac{F_o L^2}{t} \tag{7}$$

where F_o is the Fourier number for diffusion; L is the half-thickness of the crop (m); t is the drying time (s). The Fourier number is estimated using Equation (8):

$$F_o = -0.212 - 0.0101424\ln(\text{MR}) \tag{8}$$

where MR is the moisture ratio. According to Gumus and Banigo [20] and Owusu-Sekyere et al. [14], the moisture ratio is estimated using Equation (9):

$$\text{MR} = \frac{\text{MC}_t}{\text{MC}_i} \tag{9}$$

where MC_t is the moisture content at any given time.

2.4. Performance evaluation of the dryer

To analyse the high and low temperature agro-dryer performance, temperature probes are placed at critical points to measure air temperature changes during the drying process as shown in Figure 4. The arrows in the figure represent the drying flow path while the numbers represent temperature probe positions.

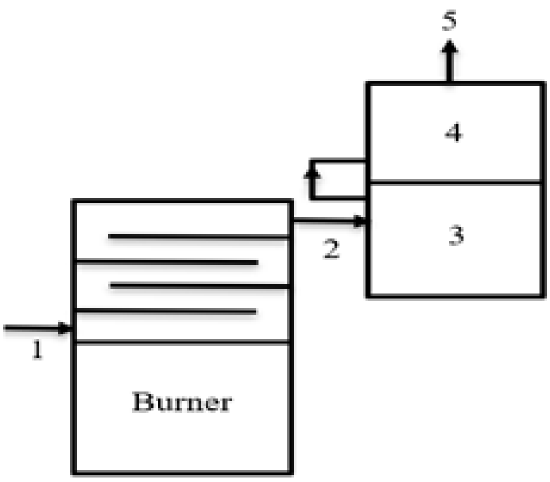

Figure 4: Temperature probe positions in the dryer.

The efficiency of the high-temperature chamber assesses how effectively the thermal energy supplied from the biomass burner is utilised to raise the drying air temperature. The high chamber efficiency is computed using Equation (10) [4, 12]:

$$\eta_H = \frac{T_2 - T_3}{T_2 - T_1} \tag{10}$$

where T_3 is the high chamber temperature (K).

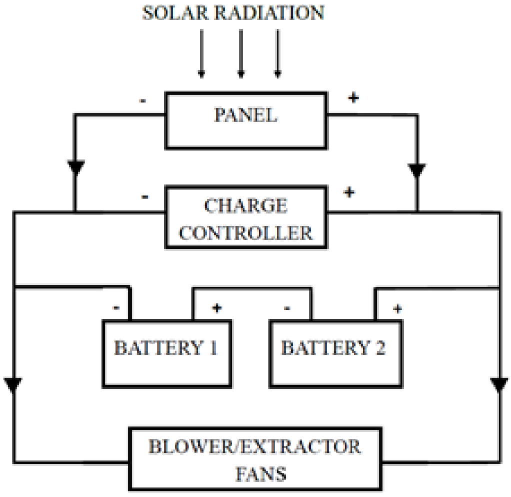

(a) Component circuit diagram

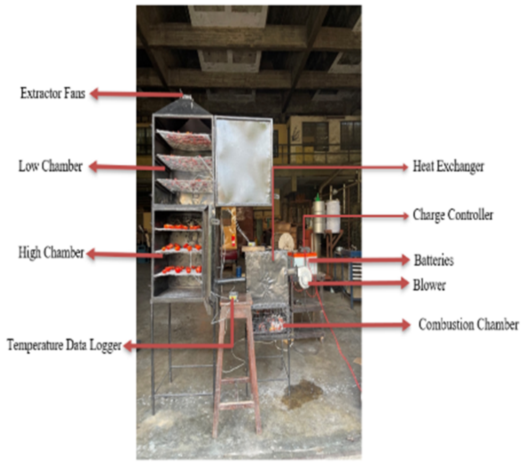

(b) Tomatoes and pepper drying

(c) SPV200M Solar Panels

(d) Weighing Scale

(e) TM 902C Temperature meter

(f) MTM-380SD Temperature meter

(g) SM206-Solar power meter

(h) RH300 Psychrometer

Figure 5: Test Rig

Since the low-temperature chamber receives preheated air from the high chamber, its performance depends on residual heat. The efficiency is therefore defined relative to the temperature drop between the outlet and inlet of the high chamber using Equation (11) [28]:

$$\eta_L = \frac{T_4 - T_5}{T_2 - T_1} \tag{11}$$

where T_4 is the low chamber temperature (K) and T_5 is the exhaust air temperature (K).

The burner efficiency measures how effectively the combustion of charcoal transfers energy to the drying air. It is calculated using Equation (12) [4, 12]:

$$\eta_B = \frac{m_a C_{pa}(T_1 - T_2)}{m_b \, \mathrm{LHV}} \tag{12}$$

The overall efficiency reflects the system's total heat utilisation from combustion through both chambers. It can be expressed as a product of the three stage efficiencies as in Equation (13) [4]:

$$\eta_o = \eta_H \times \eta_L \times \eta_B \tag{13}$$

A model of the high and low temperature agro-dryer was developed and tested. The experimental phase involved three drying tests; each focused on a unique pair of perishable agricultural products. These combinations were carefully chosen to represent a range of moisture contents and temperature sensitivity. Each test ran for eight hours from 9:00 am to 5:00 pm on separate days. The chamber selection for each crop was based on preliminary literature findings about their optimal drying conditions, with heat-sensitive crops placed in the low chamber and more thermally resilient crops in the high chamber. To evaluate the dryer's performance, temperature probes were placed at critical positions in the dryer, while also measuring the mass of the produce over a time interval of one hour. The drying air temperatures were monitored using K-type thermocouples connected to two digital thermocouple meters TM-902C and MSD380SD. A digital RH300 psychrometer and solar power meter SM 206 were used to monitor the ambient conditions. The blower and extraction fans are connected to two storage batteries in series, which are in turn continuously charged using two SPV200M solar panels in series and via BSC6048 charge controller.

Figure 5 shows a diagrammatic electrical circuit connection of the components of the dryer and the test rig.

3. Results and discussion

3.1. Drying of Tomatoes, Pepper, Onions, Bitter-leaf, Fish, Plantain

The high and low agro-dryer was tested using tomatoes and pepper in the high and low chambers respectively on 5 August 2025, termed day 1. Onions and bitter-leaf in the high and low chambers were experimented respectively on 8 August 2025, termed day 2. Testing for fish and plantain in the high and low chambers respectively was on 20 August 2025, termed day 3. The entire test spanned eight hours between 9 am to 5 pm. Figure 6 shows the before and after drying of the respective agricultural products.

Figure 6: Dried crops after eight hours.

As drying progressed, visible shrinkage and moisture loss were observed in the crops. The crops became significantly reduced in size with the passage of time. Table 5 details the moisture content of the dried crops after eight hours of drying obtained using Equation (5).

Table 5: Moisture content after drying.

Crop	Moisture Content (%)
Tomatoes	16
Pepper	6
Onions	21
Bitter-leaf	8
Herring Fish	11
Plantain	14

The outcome of the experimental testing confirms that the biomass high and low temperature cabinet dryer is suitable for the dehydration of high and low moisture content agricultural produce and demonstrates the efficacy of the dryer in handling diverse produce.

3.2. Energy transfer in heat exchanger

The thermal energy absorbed by the drying air in the heat exchanger is as shown in Figure 7 for the three test days. The fluctuations in the heat transfer are due to the uneven combustion of the biomass in the combustion chamber, varying between 4.3–4.55 kW, reflecting the sensitivity of the logarithmic mean temperature difference to fluctuations in inlet and outlet temperatures, even when the plate temperature remained constant at 800 °C. Notably, the difference between the thermal energy across the three days was within ±0.1 kW, indicating that the system maintained a relatively stable thermal performance under varying atmospheric conditions. The predicted values of heat transfer rate align well with theoretical expectations for forced convection over flat surfaces at comparable operating conditions, similar to studies by Ndukwu et al. [29] and Muritala et al. [15]. The slight variations across days are consistent with the experimental inlet and outlet air temperatures. The relatively narrow range of heat transfer rates further validates that the system was not strongly influenced by ambient fluctuations, but rather by the imposed boundary condition of plate temperature, as expected for controlled drying experiments.

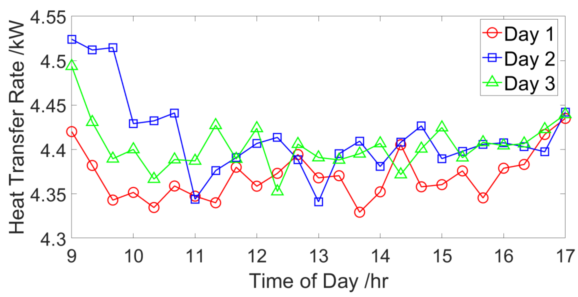

Figure 7: Thermal energy absorbed by the drying air in the heat exchanger.

3.3. Temperature variation during the course of drying

Figure 8 illustrates the inlet dry and wet temperature; heat exchanger air exit temperature; high and low chamber temperature; and exit dry and wet air temperature of the dryer during the drying of day 1, day 2 and day 3 respectively, from 9:00 am to 5:00 pm.

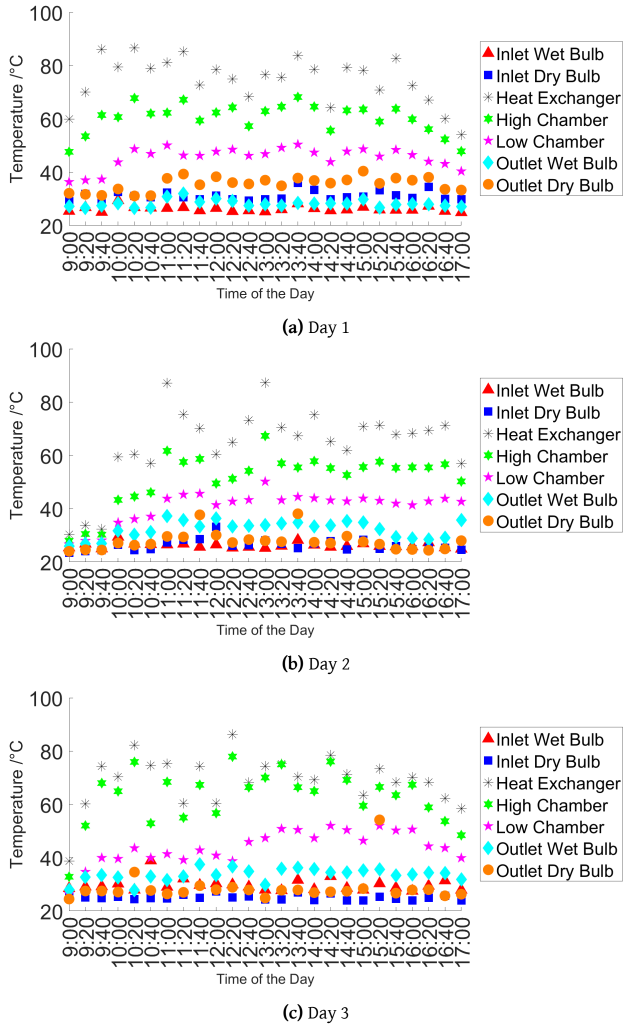

(a) Day 1

(b) Day 2

(c) Day 3

Figure 8: Temperature variation vs time in the dryer

The heat exchanger air exit temperature, peaking at 87 °C, 85 °C and 85 °C for day 1, day 2 and day 3 respectively, confirms its role as the system's thermal core. A consistent thermal gradient was observed between the high and low chambers, with average peaks of 69 °C and 52 °C, 60 °C and 45 °C, 75 °C and 55 °C respectively for day 1, day 2 and day 3, indicating effective heat transfer and controlled stratification. The inlet wet bulb temperature remained lower than the outlet, indicating the capacity of the air to absorb moisture from the agricultural product, with the higher outlet wet bulb indicating the increase in humidity of the air because of the moisture absorbed from the produce. These temperature gradients are indicative of energy utilisation in the dryer. Similar profiles align with the findings of Schmid et al. [7], Chantasiriwan [6], and Donoso-García et al. [30].

3.4. Mass and moisture loss of agricultural products

Figure 9 shows the total weight and dehydration that occurred during drying. As expected, the weight of the produce declined with each passage of time and expectedly the amount of moisture evaporated increases with time. The obtained dehydration per produce are 0.71, 0.16, 1.02, 0.2, 0.56 and 0.56 kg for tomatoes, pepper, onions, bitter-leaf, fish and plantain respectively. Ezurike et al. [11], Krokida et al. [31], and Schmid et al. [7] reported similar drying behaviour in their work. The drying rate for the respective produce are 0.08875, 0.02, 0.1275, 0.025, 0.07 and 0.07 kg/h for tomatoes, pepper, onions, bitter-leaf, fish and plantain respectively.

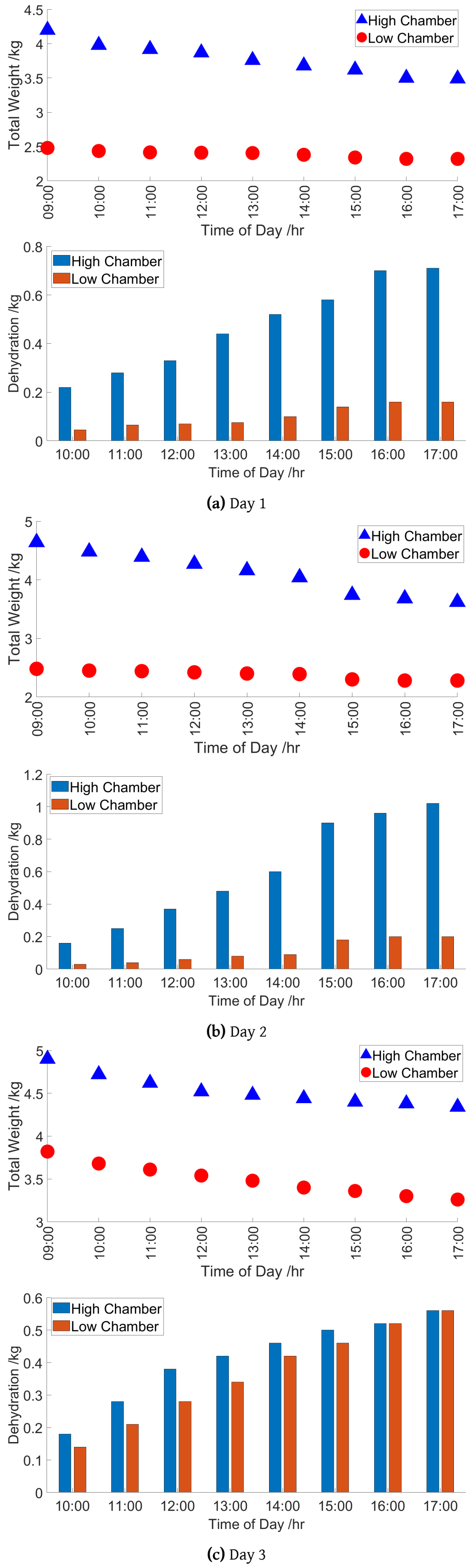

(a) Day 1

(b) Day 2

(c) Day 3

Figure 9: Total weight and dehydration vs time

3.5. Effective moisture diffusivity

Figure 10 shows how the effective moisture diffusivity of the crop samples varies against time of day. At the start of drying, all crops showed relatively high diffusivity values, which then decreased gradually over time. This occurred because water near the surface was removed quickly at the beginning, while moisture trapped inside the material moved more slowly as drying continued. Fish had the highest diffusivity because of its high moisture content and porous structure. Tomato and onion followed moderate patterns, while pepper and vegetables showed lower diffusivity due to their denser tissues. Plantain showed a smoother and more stable decline across the drying period. Overall, the trend shows that moisture diffusivity decreases with time as drying progresses. The computed values in the order of 10^{-10} m^2/s are typical for agricultural products. Similar patterns were reported by Zeng et al. [26], who observed that diffusivity increases with temperature and decreases with thickness during tea-leaf drying, and by Younis et al. [27], who found that garlic slices under infrared drying also showed decreasing diffusivity over time. The similarity in both value range and drying behaviour confirms that the results in this research are realistic and consistent with previous findings.

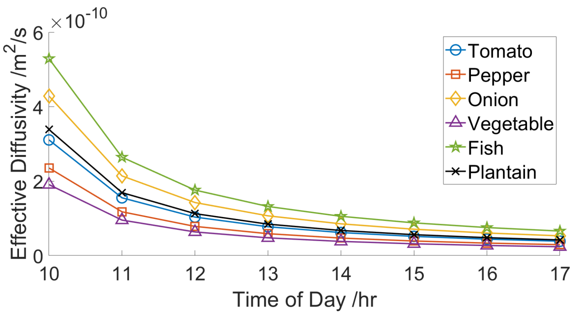

Figure 10: Moisture diffusivity vs time for the crop samples.

3.6. Drying efficiency

Figure 11 presents the temporal variation of drying efficiency across the high chamber, low chamber, and overall system for day 1, day 2 and day 3 with respect to time respectively. The peak efficiency for the high and low chamber for day 1 are 45% and 35%, for day 2 50% and 47%, and for day 3 45% and 35%, representing energy utilisation absorbed by the drying air leaving the combustion heat exchanger. The overall efficiencies for day 1, day 2 and day 3 are 12%, 15% and 12% respectively. Validation of this efficiency trend aligns with findings reported by Donoso-García et al. [30] and Murugan et al. [4], who observed similar high-chamber stability and delayed peak efficiency in lower or auxiliary drying chambers of hybrid solar dryers. Moreover, Reyes et al. [32] also documented higher efficiency phases aligning with optimal drying rate windows.

3.7. Solar irradiation variation

Figure 12 illustrates the pattern of solar radiation incident on the photovoltaic panel generating continuous electrical energy stored in the battery bank used to operate the blower and extractor fans throughout the drying period for day 1, day 2, and day 3 respectively. The solar irradiation data were monitored using the SM206 Solar Power Meter shown in Figure 5. The peak solar radiations are 600 W/m^2, 1180 W/m^2 and 400 W/m^2 for day 1, day 2 and day 3 respectively. The irregular dips observed likely result from transient cloud cover or atmospheric attenuation, as expected. These solar irradiation values incident on the photovoltaic panel generate electricity that is continuously stored in batteries that power the blower and extractor fans responsible for the circulation of drying air in the high and low agro-dryer. These solar profiles are consistent with the diurnal trend reported by Otieno et al. [33], Kumara et al. [5], Ndirangu et al. [34] and Ezurike et al. [11] in similar tropical environments, where solar insolation drives peak drying activity around noon.

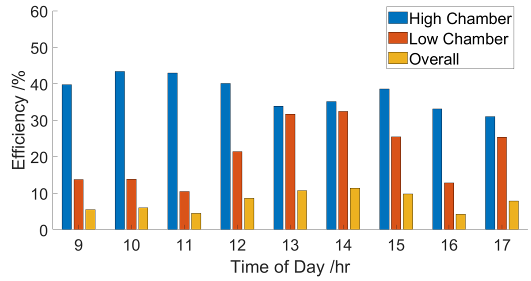

(a) Day 1

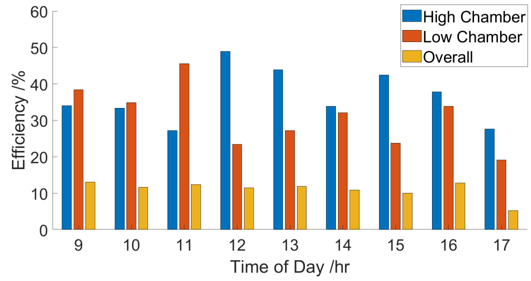

(b) Day 2

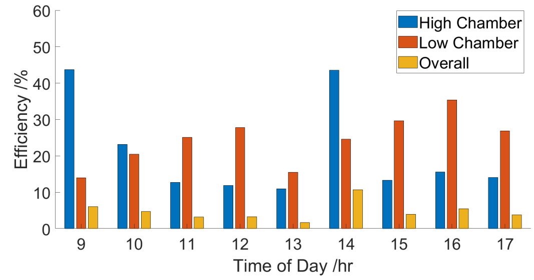

(c) Day 3

Figure 11: Efficiency vs time of the dryer

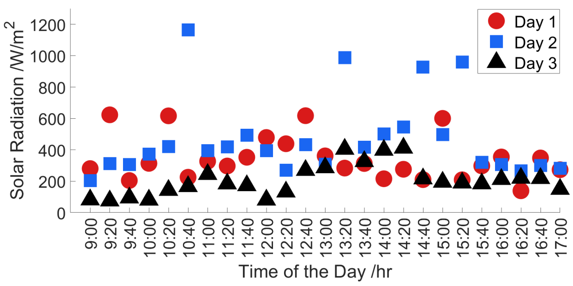

Figure 12: Solar irradiation vs time of day.

4. Conclusion

This research has developed and presented a performance evaluation of a biomass-powered high and low temperature dryer through the experimental drying of tomatoes, peppers, onions, bitter-leaf, fish and plantain. The system operated for eight hours between the hours of 9:00 am and 5:00 pm on 5, 8 and 20 August 2025. The primary objective was to assess the dryer's thermal efficiency, operational stability, and suitability for drying agricultural produce under variable environmental conditions. The drying rate for the respective produce are 0.08875, 0.02, 0.1275, 0.025, 0.07 and 0.07 kg/h for tomatoes, pepper, onions, bitter-leaf, fish and plantain respectively, with the high chambers experiencing higher drying rates than the low chambers due to their higher temperatures. Temperatures varied significantly in the course of the drying due to the irregular combustion of the biomass; the maximum recorded temperature in the high and low chamber are 69 °C and 52 °C, 60 °C and 45 °C, 75 °C and 55 °C respectively for day 1, day 2 and day 3. Analysis of the drying chambers revealed noticeable variations in thermal efficiency as expected. Peak high-chamber efficiency was 49% and consistently exceeded the low-chamber peak of 35%, while overall system efficiency peaked at 15%. These efficiency values are a function of the quantum amount of energy absorbed by the drying air in the combustion chamber. Results showed that the diffusivity of each of the crop samples decreased steadily with time, indicating that surface water evaporated quickly early in the process, while bound water removal dominated later. Average diffusivity values ranged between 1.57×10^{-10} m^2/s for bitter-leaf and 4.88×10^{-10} m^2/s for fish, with tomato, onion, pepper, and plantain falling within this interval. This demonstrates that the developed biomass high and low cabinet dryer is both functional and efficient for multi-crop drying applications under tropical sunlight conditions.

Nomenclature

A_o	surface area of flow (m^2)
c_a	specific heat of air (J/kgK)
D_{eff}	diffusivity (m^2/s)
F_o	Fourier number for diffusion
L	half-thickness of the crop (m)
LHV	lower heating value of biomass (kJ/kg)
m_a	mass of air (kg)
m_b	mass of biomass (kg)
m_i	initial mass of product before drying (kg)
m_w	mass of water evaporated per kg of product
MR	moisture ratio
MC_i	initial moisture content (%)
MC_f	final moisture content (%)
MC_t	moisture content at any given time (%)
Q	blower flow rate (m^3/s) or drying thermal energy (J)
t	drying time (s)
T_1	heat exchanger inlet temperature (K)
T_2	heat exchanger exit temperature (K)
T_3	high chamber temperature (K)
T_4	low chamber temperature (K)
T_5	exhaust air temperature (K)
U	overall heat transfer coefficient (W/m^{2}K)
w_d	final mass of dried crop after drying (kg)
w_w	mass of water removed during drying (kg)
ρ_a	air density at drying conditions (kg/m^3)
ΔT_{lm}	log-mean temperature difference (K)
η_c	thermal efficiency of combustion
η_H	high chamber efficiency
η_L	low chamber efficiency
η_o	overall efficiency

References

[1] Chuatrakool W., Achariyaviriya S., Achariyaviriya A., Moran J. C. (2020). Development of a biomass energy dryer assisted with solar energy for farmers in off-grid communities. *E3S Web of Conferences*, 187, pp. 1–8. https://doi.org/10.1051/e3sconf/202018703004

[2] Delgado-Plaza E., Peralta-Jaramillo J., Quilambaqui M., Gonzalez O., Reinoso-Tigre J., Arevalo A., Arancibia M., Paucar M., Velázquez-Martí B. (2019). Thermal evaluation of a hybrid dryer with solar and geothermal energy for agroindustry application. *Applied Sciences*, 9, 4079, pp. 1–15.https://doi.org/10.3390/app9194079

[3] Onoroh F., Ogbonnaya M., Onochie U. P. (2023). Development of a multi-agricultural products dryer using biomass. *Agricultural Engineering International: CIGR*, 25(3), 223–236.

[4] Murugan P., Dhanushkodi S., Sudhakar K., Wilson V. H. (2021). Industrial and small-scale biomass dryers: an overview. *Energy Engineering*, 118(3), pp. 435–446. https://doi.org/10.32604/ee.2021.013491.

[5] Kumara M. A. S. U., Jayewardene H. S., Jayathunga K. G. L. R., Senanayake D. P., Palipane K. B. (2006). Development and performance evaluation of a dual heat dryer: a renewable energy technology for sustainable processing of agro-produce. *Engineer*, 39(1), 19–26. https://doi.org/10.4038/engineer.v39i1.7175.

[6] Chantasiriwan S. (2023). Reduction in fuel consumption in biomass-fired power plant using hybrid drying system. *Energies*, 16, 6225, pp. 1–14. https://doi.org/10.3390/en16176225.

[7] Schmid B., Navalho S., Schulze P. S. C., Van De Walle S., Van Royen G., Schüler L. M., Maia I. B., Bastos C. R. V., Baune M. C., Januschewski E., Coelho A., Pereira H., Varela J., Navalho J., Cavaco-Rodrigues A. M. (2022). Drying microalgae using an industrial solar dryer: a biomass quality assessment. *Foods*, 11, 1873, pp. 1–20. https://doi.org/10.3390/foods11131873.

[8] Mahajan K. M., Patil V. H., Koli T. A. (2024). Design analysis of an innovative solar biomass hybrid dryer for drying turmeric. *Interactions*, 245, pp. 145–155.

[9] Sinon S., Tera S., Haro K., Djanfar E.-M., Sanogo O., Kam S. (2023). Experimental study and modeling of a convective dryer for fruits and vegetables. *Engineering*, 15, pp. 13–23. https://doi.org/10.4236/eng.2023.151002.

[10] Akowuah J. O., Maier D., Opit G., McNeill S., Armstrong P., Campabadal C., Ambrose K., Obeng-Akrofi G. (2018). Drying temperature effect on kernel damage and viability of maize dried in a solar biomass hybrid dryer. *Open Journal of Applied Sciences*, 8, 506–517. https://doi.org/10.4236/ojapps.2018.811041.

[11] Ezurike B. O., Abid M., Ajah S. A., Okoronkwo C. A., Adun H., Nwawelu U. N., Bamisile O., Zaini J. H. (2023). Design and numerical energetic analysis of a novel semi-automated biomass-powered multipurpose dryer. *Sustainability*, 15, 6639, pp. 1–14. https://doi.org/10.3390/su15086639.

[12] Çengel Y. A., Ghajar A. J. (2015). *Heat and Mass Transfer Fundamentals and Application* (5th ed.). McGraw-Hill Education, pp. 145–640.

[13] Famurewa J. A. V., Adejumo P. O., Adejumo A. O. (2017). Performance evaluation of a biomass fuelled cabinet dryer. *Open Academic Journal of Advanced Science and Technology*, 1(1), pp. 12–19. https://doi.org/10.33094/5.2017.11.12.19.

[14] Owusu-Sekyere E., Obeng-Akrofi G., Akowuah J. O., Maier D. (2021). Performance analysis and drying kinetics of maize in an AflaSTOP dryer. *Open Journal of Applied Sciences*, 11, pp. 327–342. https://doi.org/10.4236/ojapps.2021.113024.

[15] Muritala A. O., Odediran S. O., Obayopo S. O., Adio S. A. (2022). A study of a forced convective biomass dryer for plantain chips. *Agricultural Engineering International: CIGR Journal*, 24(4), pp. 209–218.

[16] Mercer D. G. (2014). Part 2: *An introduction to the dehydration and drying of fruits and vegetables*. University of Guelph, pp. 1–129.

[17] Oboh F. O. J., Masodje H. I. (2009). Nutritional and antimicrobial properties of *Vernonia amygdalina* leaves. *International Journal of Biomedical and Health Sciences*, 5(2), pp. 51–56.

[18] Walker S. J. (2011). *Postharvest handling of dehydrated chiles, Guide H-236*. New Mexico State University, Cooperative Extension Service, pp. 1–4.

[19] Olafsdottir G., Margeirsson B. (2014). *Effect of different drying methods on the quality and shelf life of herring fillets*. United Nations University Fisheries Training Programme (UNU-FTP), Iceland. https://www.grocentre.is/static/gro/publication/16/document/won_08fued.pdf. Retrieval date: 30 July 2025.

[20] Gumus R. H., Banigo N. (2015). Drying characteristics and kinetics of bitter leaves (*Vernonia amygdalina*) and scent leaves (*Ocimum gratissimum*). *Chemical and Process Engineering Research*, 32, pp. 1–11.

[21] Jayeeta M., Shrivastava S. L., Rao P. S. (2012). Onion dehydration: a review. *Journal of Food Science and Technology*, 49(3), pp. 267–277. https://doi.org/10.1007/s13197-011-0369-1.

[22] Reeb J., Milota M. (1999). Moisture content by the oven-dry method for industrial testing. In *Proceedings of the 50th Western Dry Kiln Association Meeting*, pp. 66–74.

[23] Sweelem E. A., Nafeh A.-S. A., Fahmy F. H. (2013). Sizing and design of the PV-wind energy dryer for medical herbs. *Smart Grid and Renewable Energy*, 4, pp. 217–226. http://dx.doi.org/10.4236/sgre/2013.42027.

[24] King'ori E., Simate I. N. (2024). Design and development of a parabolic trough solar air heater for a greenhouse dryer. *Journal of Power and Energy Engineering*, 12, pp. 1–18. https://doi.org/10.4236/jpee.2024.129001.

[25] Bola F. A., Bukola A. F., Olanrewaju I. S., Adisa S. B. (2013). Design parameters for a small-scale batch in-bin maize dryer. *Agricultural Sciences*, 4(5B), pp. 90–95.https://doi.org/10.3389/fsufs.2024.1371696.

[26] Zeng Z., Han C., Wang Q., Yuan H., Zhang X., Li B. (2024). Analysis of drying characteristic, effective moisture diffusivity and energy, exergy and environment performance indicators during thin layer drying of tea in a convective-hot air dryer. *Frontiers in Sustainable Food Systems*, 8, pp. 1–13. https://doi.org/10.3389/fsufs.2024.1371696.

[27] Younis M., Abdelkarim D., Zein El-Abdein A. (2018). Kinetics and mathematical modeling of infrared thin-layer drying of garlic slices. *Saudi Journal of Biological Sciences*, 25, pp. 332–338. http://dx.doi.org/10.1016/j.sjbs.2017.06.011.

[28] Desai P. S. (2004). *Modern Refrigeration & Air Conditioning*. Khanna Publishers, pp. 250–490.

[29] Ndukwu M. C., Diemuodeke E. O., Abam F. I., Abada U. C., Ekeemezie N., Simo-Tagne M. (2020). Development and modelling of heat and mass transfer analysis of a low-cost solar dryer integrated with biomass heater: application for West African Region. *Scientific African*, 10, pp. 1–12. https://doi.org/10.1016/j.sciaf.2020.e00615.

[30] Donoso-García P., Henríquez-Vargas L., González J., Díaz I., Fuentes I. (2024). A study for estimating the overall heat transfer coefficient in a pilot-scale indirect rotary dryer. *Processes*, 12, 357, pp. 1–19. https://doi.org/10.3390/pr12020357

[31] Krokida M. K., Karathanos V. T., Maroulis Z. B., Marinos-Kouris D. (2003). Drying kinetics of some vegetables. *Journal of Food Engineering*, 59, pp. 391–403. https://doi.org/10.1016/S0260-8774(02)00498-3

[32] Reyes A., Cubillos F., Mahn A., Vásquez J. (2014). Dehydration of agro products in a hybrid solar dryer controlled through a fuzzy logic system. *International Journal of Modern Nonlinear Theory and Application*, 3, pp. 66–76. http//dx.doi.org/10.4236/ijmnta.2014.33009.

[33] Otieno A. O., Home P. G., Raude J. M., Murunga S. I., Gachanja A. (2022). Heating and emission characteristics from combustion of charcoal and co-combustion of charcoal with faecal char-sawdust char briquettes in a ceramic cook stove. *Heliyon*, 8, pp. 1–8. https://doi.org/10.1016/j.heliyon.2022.e10272

[34] Ndirangu S. N., Ronoh E. K., Kanali C. L., Mutwiwa U. N., Kituu G. M. (2020). Design and performance evaluation of a solar-biomass greenhouse dryer for drying selected crops in western Kenya. *Agricultural Engineering International: CIGR Journal*, 22(3), pp. 219–229.